

PION-⁴He SCATTERING AROUND THE $\frac{3}{2}, \frac{3}{2}$ RESONANCE

F. Binon^{*)}, P. Duteil^{**)}, M. Gouanère^{***)}, L. Hugon^{†)},
J. Jansen^{**)}, J-P. Lagnaux^{*)}, H. Palevsky^{††)},
J-P. Peigneux^{***)}, M. Spighel^{***)}, J-P. Stroot^{*)}

IISN (Belgium)-IPN (Orsay) Collaboration

ABSTRACT

π^- -⁴He differential cross-sections at 110, 150, 180, 220 and 260 MeV as well as total cross-sections at eleven energies between 67 and 285 MeV, are presented.

Geneva - 24 June 1975

(Submitted to Physical Review Letters)

-
- *) IISN, Belgium.
**) CERN, Geneva, Switzerland.
***) IPN, Faculté des Sciences, Orsay, France.
†) Faculté des Sciences, Clermont-Ferrand, France. Now at IUT, Montluçon, France.
††) On leave from BNL, USA.

... ..
... ..
... ..
... ..

...

... ..
... ..
... ..

...

...

... ..
... ..

...

...

... ..
... ..

...

Negative pion-⁴He scattering has been measured at the CERN SC with the double achromatic spectrometer already used for pion-¹²C scattering^{1,2}). A liquid helium target of the supercooled type with a precise temperature regulation was installed for these measurements. Its windows consisted of thin havar foils, except for the very forward angle measurements, where mylar windows were used because of their lower atomic number. Effective target thicknesses are extrapolated from window bulge measurements made at room temperature under controlled pressure conditions. The relative error of this procedure is ±3%. It is the main contribution to the total relative error on the absolute normalization of the data which is estimated to be ±4%.

Momentum dispersion of the incident pion beam was $\Delta p/p = \pm 1.8\%$. Over-all angular resolution was 1° using a set-up which included a DISC counter for identifying the forward scattered pions. It was 2° for the large-angle measurements.

The experimental data are represented in Fig. 1. Differential cross-sections are given as a function of the scattering angle in the centre-of-mass system.

Cross-sections for 180° scattering were measured by observing ⁴He nuclei recoiling in the forward direction. For this purpose, the target was filled with helium gas under pressure and temperature conditions such that recoil α -particles had still enough energy to traverse the detectors placed at the entrance of the analysing spectrometer and at its focal plane. These detectors were low-pressure multiwire proportional chambers³) filled with pentane at a pressure of 6 mm of Hg. The trajectories of the particles were in this case completely in vacuum. Unexpected difficulties arose in the absolute normalization of these data⁴). The differential cross-sections for pion scattering at 180° were finally deduced from the following scaling:

$$\left[\frac{d\sigma}{d\Omega} (180^\circ) \right]_{\text{cm}}^{\pi} = \left[\frac{d\sigma}{d\Omega} (146.8^\circ) \right]_{\text{cm}}^{\pi} \times \left\{ \left[\frac{d\sigma}{d\Omega} (0^\circ) \right]_{\text{cm}}^{\alpha} / \left[\frac{d\sigma}{d\Omega} (33.2^\circ) \right]_{\text{cm}}^{\alpha} \right\}$$

where 146.8° is the angle in the c.m. system corresponding to the maximum angle in the laboratory at which the spectrometer could be rotated, namely 144° , and 33.2° is the corresponding angle in the c.m. for the recoiling alphas.

Total cross-sections are represented in Fig. 2, together with results from Wilkin et al.⁵). Measurements were made with a set of five scintillation counters with increasing diameters placed right behind the target inside the scattering chamber. The pions were signed with a DISC counter placed just before the scattering chamber. The target was a hollow copper cylinder, 80 mm in diameter and 60 mm long, covered with thin havar windows filled with liquid helium. Coulomb-nuclear interference effects were corrected for by using the ratio

$\rho = \text{Re } f(0)/\text{Im } f(0)$ as deduced from our elastic-scattering data. In Fig. 2 are also shown the total elastic cross-sections obtained by integrating measured angular distributions and the remaining total inelastic cross-sections. Points at 51 MeV, 60 MeV, 68 MeV and 75 MeV are deduced from the data of Crowe et al.⁶⁾. Enough positive pions were available at 110 MeV for a total cross-section to be made at this energy. The curve in Fig. 2 is a theoretical prediction by Locher⁷⁾.

Total cross-sections agree with those of Wilkin et al. except for the lowest energies where the discrepancy is outside experimental errors.

Differential cross-sections smoothly continue the low-energy data of Crowe et al.⁶⁾, but they show very novel features. Firstly, the angular position of the first minimum is independent of the pion incident energy, whereas the first minimum takes place at approximately constant t in the pion-¹²C case. It probably means that in the ⁴He case, this minimum is connected to the zero of the non-spin flip π -N amplitude rather than being of a diffractive nature. Secondly, another minimum, which is wider than the first one, appears at 150 MeV and it moves towards smaller angles as the pion energy increases. Moreover, the height of the second maximum decreases by two orders of magnitude when the pion energy goes from 110 to 260 MeV, across the (3,3) resonance, whereas it remains almost constant in the ¹²C case¹⁾.

The measured differential cross-sections are fitted with the expression:

$$\frac{d\sigma}{d\Omega} = \left| f_N e^{-i2\delta} + f_C \right|^2 .$$

f_N , f_C , and 2δ are respectively the nuclear scattering amplitude, the Coulomb amplitude and a standard Bethe phase^{2,8)}. Following a suggestion made by Germond and Wilkin, a form of $f_N(t)$ is chosen as:

$$f_N(t) = \frac{k}{4\pi} \sigma_{\text{tot}} [i + \rho] \exp \left[+ \frac{R_S^2}{6} t \right] \prod_j \left(1 - \frac{t}{t_j} \right) ,$$

where t_j 's are complex numbers. The number of factors in the product \prod_j is taken to be equal to the number of dips in the angular distributions, i.e. one at 110 MeV and below, two at 150 MeV and above. Fitted values of the parameters are given in Table 1. The sign of the imaginary parts will be explained in the final paper⁴⁾, as it results from a choice and is not forced on us. Equally good fits can be obtained with the reverse sign.

From the values of Table 1 it is easy to deduce R , the slope at zero momentum transfer. The obtained values are fitted with an effective radius model formula^{9,10)}, $R^2 = R_A^2 + a/k^2$ [where a equals $\frac{3}{2} \ell(\ell + 1)$ if one partial wave predominates]. One gets $R^2 = (1.55 \pm 0.03)^2 + (4.40 \pm 0.12)/k^2$ which is compatible with a dominant p-wave interaction.

In Fig. 3 are shown the values of the real part of the forward scattering amplitude $\text{Re } f(0) = \rho \cdot (k/4\pi) \sigma_{\text{tot}}$ plotted versus T . Values at 51 MeV, 60 MeV, 68 MeV, and 75 MeV were obtained by analyzing Crowe data⁶⁾ in the way described above by using values of σ_{tot} extrapolated down to 51 MeV. The curves are forward dispersion relation calculations made by Wilkin⁵⁾ and by Batty¹¹⁾.

We are greatly indebted to Drs. J.F. Germond and C. Wilkin for many fruitful discussions concerning the interpretation of the data. The helium target was built in the Cryogenic Department at IPN (Orsay). We are very grateful to its chief Mr. S. Buhler, and to Mr. J. Mommejat for their devoted assistance. We thank the CERN SC operators. We enjoyed the help of Dr. V. Bobyr during the early part of the experiment and of Dr. E. Labie during the last runs.

REFERENCES

- 1) F. Binon, P. Duteil, J.P. Garron, J. Görres, L. Hugon, J.P. Peigneux, C. Schmit, M. Spighel and J.P. Stroot, Nuclear Phys. B17, 168 (1970).
- 2) F. Binon, V. Bóbyr, P. Duteil, M. Gouanère, L. Hugon, J.P. Peigneux, J. Renuart, C. Schmit, M. Spighel and J.P. Stroot, Nuclear Phys. B33, 42 (1971), and Erratum: Nuclear Phys. B40, 608 (1972).
- 3) F. Binon, V. Bobyr, P. Duteil, M. Gouanère, L. Hugon, M. Spighel and J.P. Stroot, Nuclear Instrum. Methods 94, 27 (1971).
- 4) F. Binon et al., to be published.
- 5) C. Wilkin, C. Cox, J. Domingo, K. Gabathuler, E. Pedroni, J. Rohlin, P. Schwaller and N. Tanner, Nuclear Phys. B62, 61 (1973).
- 6) K. Crowe, A. Fainberg, J. Miller and A. Parsons, Phys. Rev. 180, 1349 (1969).
- 7) M. Locher, O. Steinmann and N. Straumann, Nuclear Phys. B27, 598 (1971).
- 8) M. Locher, Nuclear Phys. B2, 525 (1967).
- 9) J. Beiner and J.F. Germond, Phys. Letters 46 B, 289 (1973).
- 10) R. Silbar and M. Sternheim, Phys. Rev. Letters 31, 941 (1973).
- 11) C. Batty, G. Squier and G. Turner, Rutherford Lab. preprint RL-73-118 (1973).

Table 1

T (MeV)	ρ	R_S (fm)	Re (1 - z ₁)	Im (1 - z ₁)	Re (1 - z ₂)	Im (1 - z ₂)	n	χ^2
110	0.560 ± 0.047	1.685 ± 0.018	0.704 ± 0.009	0.185 ± 0.010	-	-	114	126
150	0.153 ± 0.078	1.238 ± 0.131	0.729 ± 0.007	0.137 ± 0.010	2.149 ± 0.876 0.219	-0.533 ± 0.092	25	29
180	-0.023 ± 0.031	1.310 ± 0.061	0.708 ± 0.008	-0.072 ± 0.012	1.613 ± 0.024	-0.372 ± 0.055	109	129
220	-0.013 ± 0.147	1.262 ± 0.035	0.721 ± 0.005	0.020 ± 0.011	1.452 ± 0.023	-0.202 ± 0.031	23	40
260	-0.317 ± 0.028	1.341 ± 0.032	0.726 ± 0.011	0.063 ± 0.023	1.350 ± 0.026	-0.119 ± 0.051	107	91

Remark: 1 - z_j = -t_j/2k²; n is the number of degrees of freedom in the fits.

Figure captions

- Fig. 1 : π^- - ^4He elastic scattering differential cross-sections versus Θ_{cm} , the pion scattering angle in the c.m. system. Optical points * show the value of $|\text{Im } f|^2$ as deduced from our measured total cross-sections. Only part of the forward data are shown for the sake of clarity. The curves result from fits to a formula given in the text.
- Fig. 2 : π^- - ^4He total cross-sections versus T, pion kinetic energy in the laboratory system. [\times : Wilkin et al.⁵⁾, \square : deduced from data of Crowe et al.⁶⁾] The solid lines are a guide for the eye only. The dotted curve is a theoretical prediction by Locher et al.⁷⁾.
- Fig. 3 : Real part of the forward scattering amplitude versus T, pion kinetic energy in the laboratory system. The curves were calculated from the forward dispersion relation by Wilkin et al.⁵⁾ (dotted curve) and by Batty et al.¹¹⁾ (full curve).

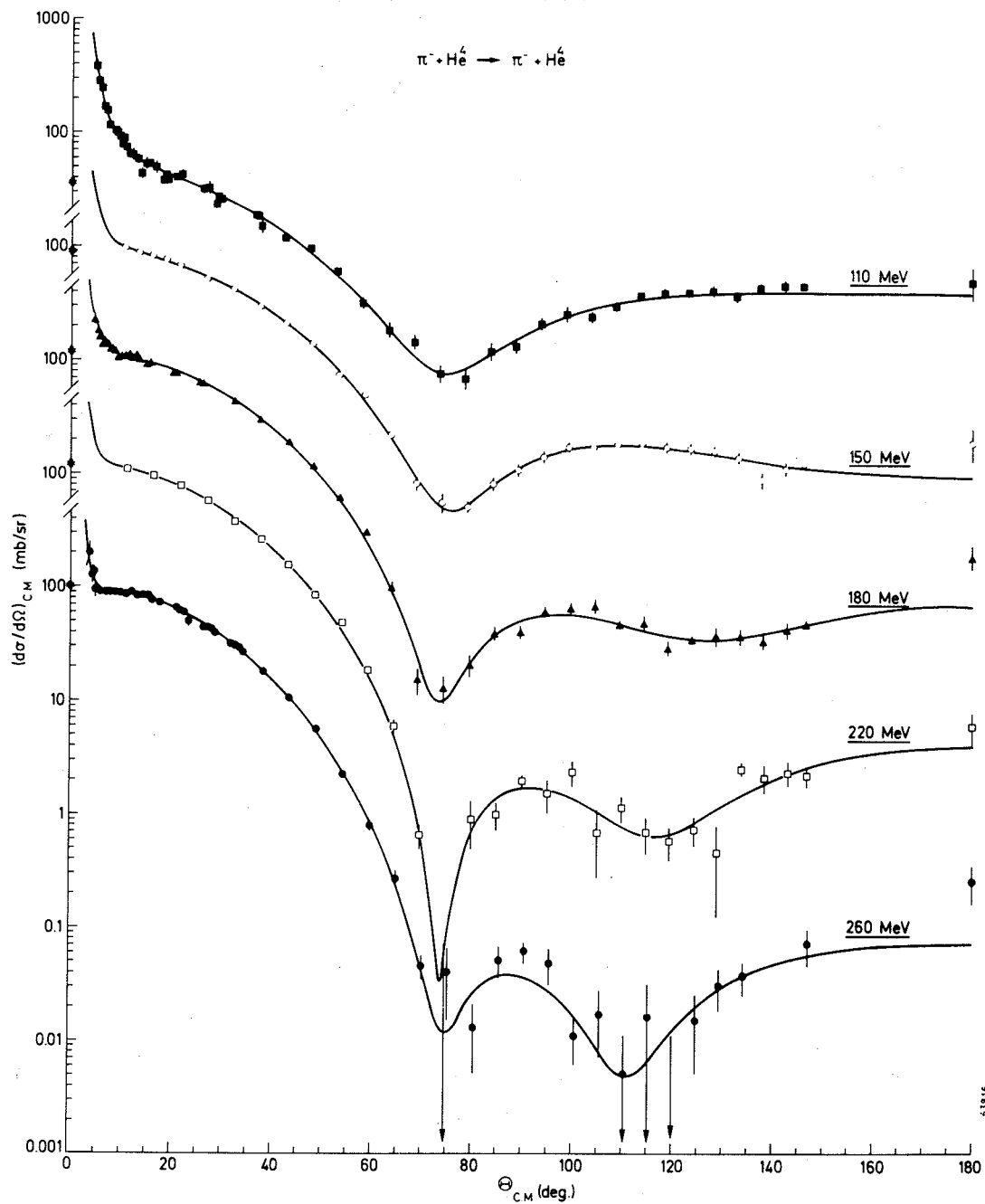


Fig.1

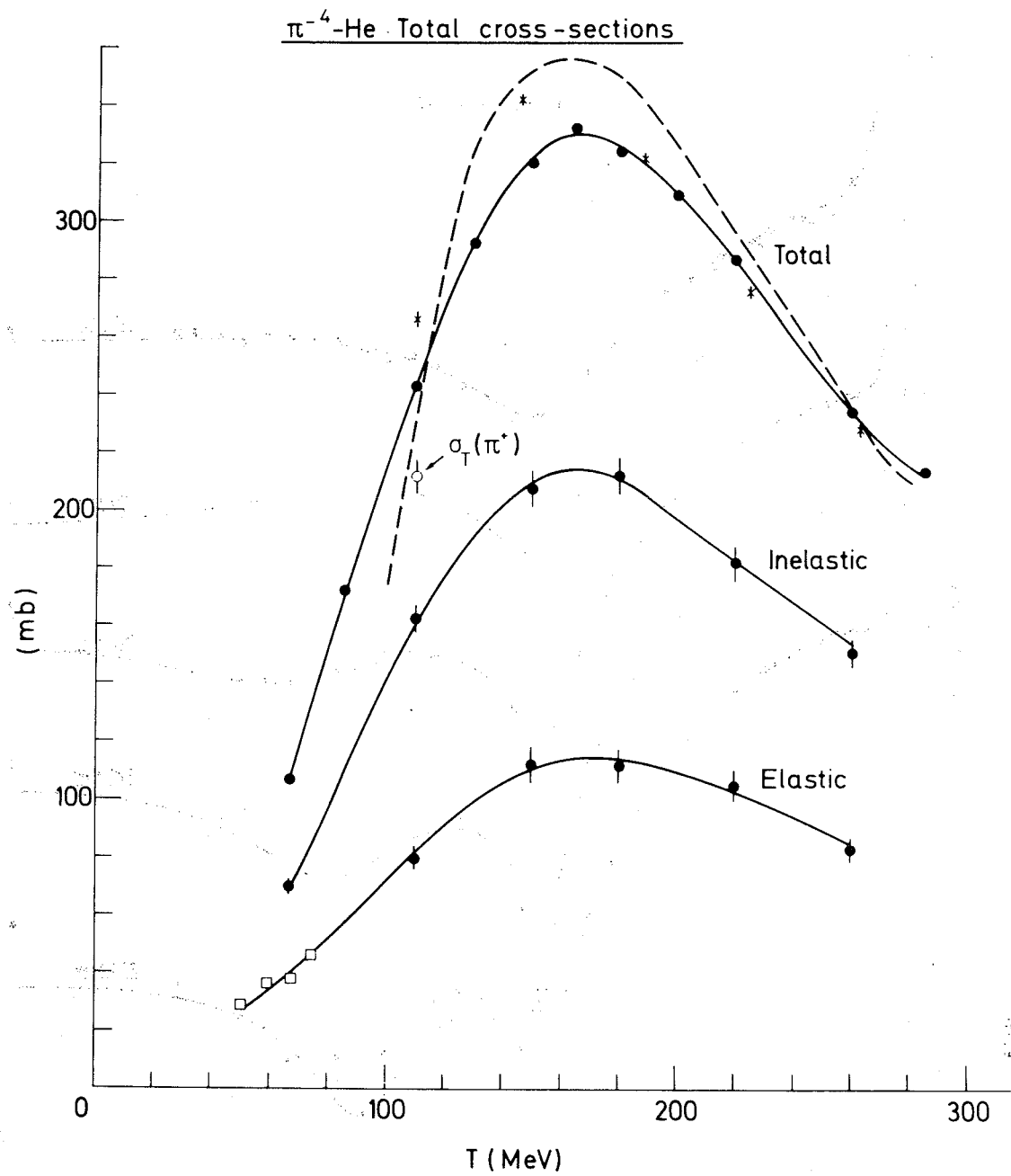


Fig. 2

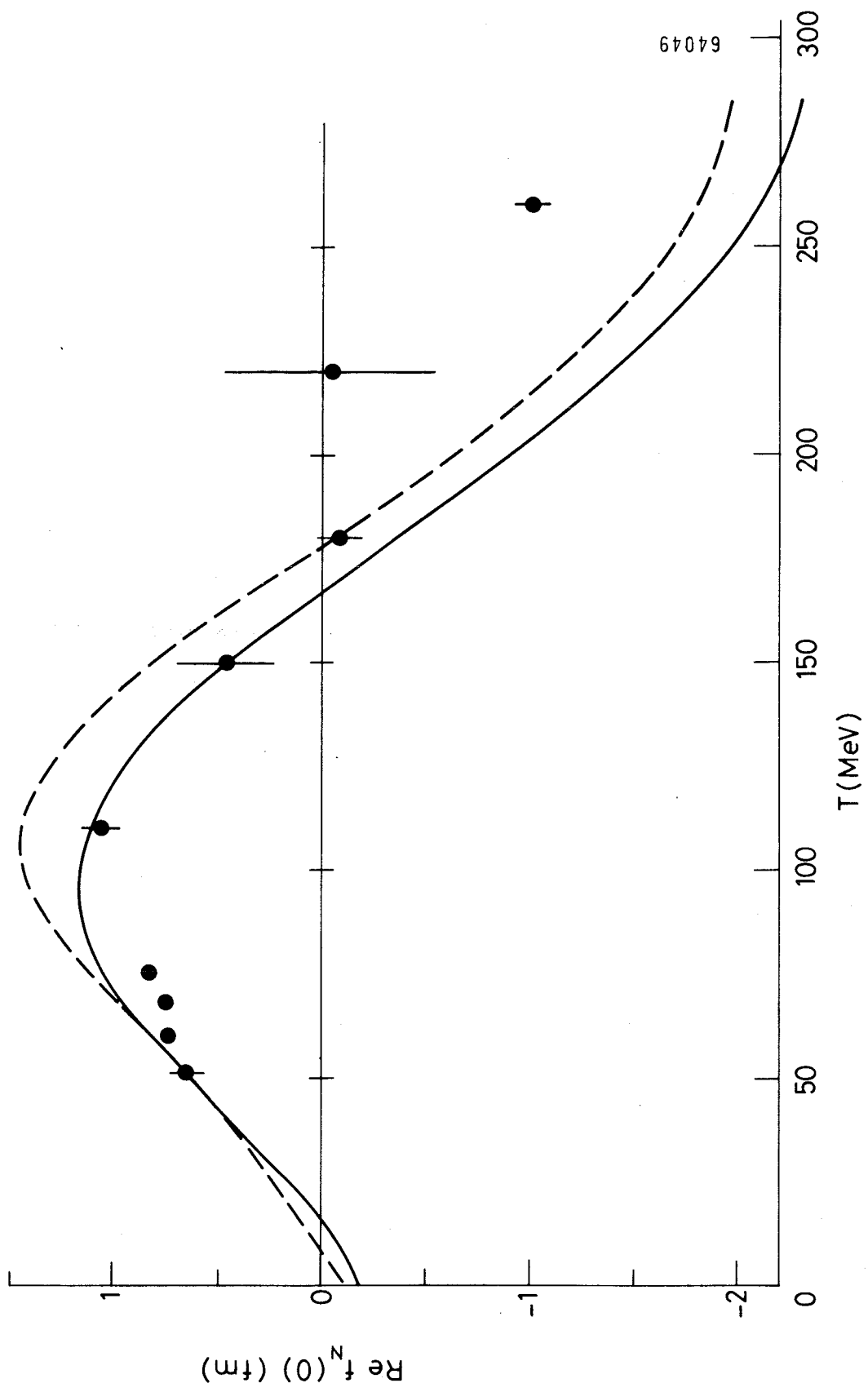


Fig. 3

